Wiley Online Library Early View publication on www.wileyonlinelibrary.com (issue and page numbers not yet assigned; citable using Digital Object Identifier – DOI)

J. Biophotonics 1–12 (2016) / **DOI** 10.1002/jbio.201600162

Journal of BIOPHOTONICS

FULL ARTICLE

Optical redox ratio and endogenous porphyrins in the detection of urinary bladder cancer: A patient biopsy analysis

Scott Palmer[1], *Karina Litvinova*[2], *Andrey Dunaev*[3], *Ji Yubo*[1], *David McGloin*[4], *and Ghulam Nabi**, [1]

[1] Division of Imaging and Technology, University of Dundee, Ninewells Hospital and Medical School, James Arrott Drive, Dundee, UK DD1 9SY
[2] Optoelectronics and Biomedical Photonics Group, Aston Institute of Photonic Technologies, Aston University, Aston Triangle, Birmingham, UK B4 7ET
[3] Biomedical Photonics Instrumentation Group, Scientific-Educational Centre of "Biomedical Engineering", Orel State University, Orel, Russia, 302020
[4] SUPA, School of Science and Engineering, Ewing Building, University of Dundee, Nethergate, Dundee, UK DD1 4HN

Received 30 May 2016, revised 10 August 2016, accepted 21 August 2016
Published online 10 October 2016

Key words: urinary bladder cancer, Transitional cell carcinoma, multifunctional laser, cancer biomarkers, detection, autofluorescence

Bladder cancer is among the most common cancers in the UK and conventional detection techniques suffer from low sensitivity, low specificity, or both. Recent attempts to address the disparity have led to progress in the field of autofluorescence as a means to diagnose the disease with high efficiency, however there is still a lot not known about autofluorescence profiles in the disease. The multifunctional diagnostic system "LAKK-M" was used to assess autofluorescence profiles of healthy and cancerous bladder tissue to identify novel biomarkers of the disease. Statistically significant differences were observed in the optical redox ratio (a measure of tissue metabolic activity), the amplitude of endogenous porphyrins and the NADH/porphyrin ratio between tissue types. These findings could advance understanding of bladder cancer and aid in the development of new techniques for detection and surveillance.

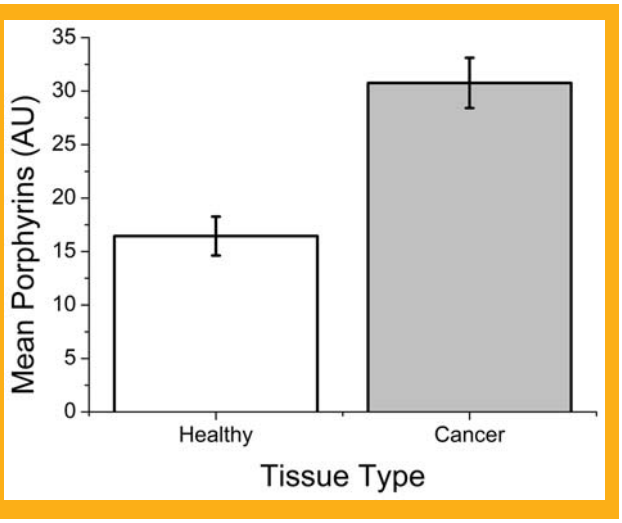

1. Introduction

Bladder cancer (BCa) is among the most common cancers [1]. BCa can be separated into non-muscle-invasive (NMIBC) and muscle-invasive (MIBC) diseases. NMIBC is contained within the urothelium (the inner epithelial layer of the bladder) and lamina propria, however high grade instances of NMIBC present with the potential to quickly transition from NMIBC to MIBC. Similarly, carcinoma *in situ* (CIS)

* Corresponding author: e-mail: g.nabi@dundee.ac.uk, Phone: (+44) 01382 660111

[2] possesses significant malignant potential to quickly progress into MIBC. BCa is conventionally detected by the gold standard white light cystoscopy (WLC) and voided urine cytology (VUC) [3] which identifies cytological abnormalities. Suspect tissue identified by WLC is confirmed by biopsy. Unfortunately, WLC and VUC suffer from low sensitivity, especially for low stage cancers such as flat NMIBC and CIS. VUC sensitivity for transitional cell carcinoma (TCC) is between 25–50% [4, 5], while WLC sensitivity for TCC ranges between 60–70% [6, 7] (but can be as low as 4% for CIS cases [8]. The result of this low sensitivity is a high rate of tumour progression and recurrence, which puts a large burden on health services each year. Bladder cancers which progress to MIBC stage can often only be adequately dealt with by radical cystectomy [9]. Steps have been taken to improve on the low sensitivity of WLC and VUC with photodynamic diagnosis (PDD) using photosensitisers (PS). These accumulate preferentially in tumour tissue due to the enhanced permeability and retention effect [10] by retaining hexaminolaevulinate (HAL) [11] and 5-aminolaevulinic acid (5-ALA) [12]. PDD is shown to improve the sensitivity of cytoscopic detection of bladder cancer compared to WLC [13] – reducing NMIBC recurrence rates [14] – but at the cost of reduced specificity due to uptake by inflamed healthy tissue previously treated by surgery or chemotherapy [7, 15]. There is a need therefore for novel detection techniques which possess high sensitivity and specificity.

Many of the molecules present in human tissue naturally fluoresce, including amino acids (tryptophan [16, 17]), structural proteins (collagen [18] and elastin [19]), metabolic cofactors (NADH [20] and flavins [21]) and blood precursors (porphyrins [22]). Tissue remodelling by tumours has previously been shown to significantly reduce local collagen levels to promote invasion and metastasis [23]. Furthermore, metabolic disparity between healthy and cancerous tissue has been extensively explained by the Warburg effect [24]. The optical redox ratio (ORR) takes into account the accumulation of NADH in cancer cells by rationing NADH content to flavin content (NADH/Flavin) to give a measure of the extent of the Warburg effect. The ORR has previously discriminated between healthy and cancerous cells [25–27], including by ourselves in bladder cancer [28]. Alfano et al. were among the first to discuss autofluorescence spectroscopy for cancer detection, applying UV fluorescence spectroscopy to the identification of breast and lung cancers [29] and characterising flavin and porphyrin fluorescence in mouse bladder tumours [30]. Autofluorescence spectroscopy for cancer diagnosis in a wide range of tissues has since been covered comprehensively [31], including for bladder cancer [32–35]. Early research comparing autofluorescence with PDD suggested that UV autofluorescence spectroscopy was a more effective tool for tumour margin demarcation than PDD [36]. D'Hallewin et al. previously reviewed the field of bladder autofluorescence spectroscopy [37], concluding that tissue thickening was the major contributor to significant differences between healthy and cancerous tissue (measured as the fluorescence of collagen and NADH), in keeping with findings from collagen/NADH ratios in prostate cancer [38] and Barrett's oesophagus [39]. A limitation of this method is its application for the detection of flat CIS, which does not cause tissue thickening. In light of this, new biomarkers and diagnostic ratios for autofluorescence detection of bladder cancer are required which are independent of tissue thickening. The limitation to our understanding of the contributions of individual fluorophores to complex tissue spectra is being addressed by contemporary research [38, 40], allowing us to better address this issue. Anidjar et al. attempted to address this by studying tryptophan fluorescence in tissue, recording diagnostic worth for CIS [41]. Recently, our group identified progressive changes in the ORR of bladder cancer organoids [42]. As the ORR is a measure of metabolic activity in cells and tissues, it may provide worth to better understand bladder autofluorescence irrespective of tissue thickening. We were therefore interested to see whether this phenomenon would be reproduced in human biopsy samples. We sought to investigate whether the decreased ORR seen in progressing bladder cancer organoids would be corroborated in human bladder tissue.

Another limitation of autofluorescence spectroscopy is scattering and absorption of UV light, impeding its penetration deeper into tissue. There is current interest in the study of tissue optical properties at longer wavelengths, into the optical window (650–950 nm) [43]. Our secondary objective, therefore, was to use longer wavelength light (635 nm) to investigate whether endogenous porphyrins can be used as a diagnostic marker of bladder cancer. Research into the relationship between porphyrin levels and bladder cancer generally relates to their accumulation during PDD, therefore the profile of endogenous porphyrin in non-sensitised tissue is poorly understood. Porphyrins have been shown to accumulate in oral cancer [44] and in the blood [22] and tissue [45] of mice bearing renal cell carcinoma. We therefore considered that endogenous porphyrins may likewise accumulate in non-sensitised human bladder tissue. Finally, we sought to corroborate previous findings by Aboumarzouk et al. [35] of a statistically significant difference in the ratio of NADH/porphyrins in bladder cancer. Our main hypotheses were: bladder cancer tissue will possess a reduced ORR, an increased endogenous porphyrin concentration and a reduced NADH/porphyrin ratio rela-

tive to healthy tissue. Our research findings confirm these hypotheses. These findings may better inform our understanding of autofluorescence analysis of bladder cancer through the corroboration of a lab-based organoid model and through the identification of a suitable cancer biomarker at a longer wavelength (endogenous porphyrins). Ultimately, these biomarkers and diagnostic ratios may help to better address shortcomings of autofluorescence diagnosis by providing new biomarkers and diagnostic ratios which are not dependent on tissue thickening. These findings also contribute to the development of a multi-functional system with which the oxygenation, blood flow and autofluorescence status of human bladder tissue can be studied simultaneously.

2. Experimental

2.1 Laser setup

The commercial unit "LAKK-M" ("Multi-functional laser analyser of capillary blood flow") (SPE-LAZMA, Moscow, Russia) was used for all fluorescence spectroscopy measurements. This facilitates multi-wavelength optical excitation and detection of fluorescence signals. The central functional unit contains the light sources used for measurements (1.5 mW 365 nm LED for UV excitation and 5.5 mW 635 nm semi-conductor laser for red excitation). The system also contains blue (450 nm) and green (532 nm) laser sources. Blue light can also be used to excite FAD fluorescence, however UV excitation is more stable for studying the optical redox ratio. Tissue fluorescence under green excitation could not be attributed to any known fluorophores so was omitted from analysis. The laser sources are connected to optical fibres and combined with their respective detection fibres into a single probe of outer assembly diameter of 2 mm (the distance separating each source from its detector being 0.5 mm), which forms the optical probe of the LAKK-M system. The probe is brought into contact with the biological object (or inserted into the cuvette for fluorophore measurements), following which the laser is switched on, incident laser light is delivered by the particular excitation fibre to the tissue, transformed by the tissue and the transformed light is received by the respective detection fibre housed 0.5 mm away. Penetration depth of light into tissue ranges between 0.5–1 mm, depending on the source used. Optical filters are used to attenuate (roughly × 1000) the intensity of back-scattered light received and displayed by the detector. The detection fibres are coupled to a charge coupled device (CCD) and an inbuilt spectrometer with polychromator and diffraction grating to detect fluorescence between 350–823 nm at 0.2 nm increments. The information from the spectrometer (fluorescence spectra including intensity of fluorescence and individual biomarker values) is displayed on the controlling laptop (to form a feedback loop) using the custom made software "LDF 3.1" (SPE-LAZMA), from which fluorescence is quantified in arbitrary units (AU) by fluorescence intensity at designated wavelengths. The setup and function of the LAKK-M system is explained in greater detail previously by Dunaev et al. [46] while the general setup is depicted in Figure 1. An example of spectral readout of UV-excited tissue fluorescence by the custom-made software is depicted in Figure 2, showing the back-scattered light, tissue fluorescence spectrum, biomarker amplitude values and the calculated diagnostic ratios. The LAKK-M system is switched on at least 30 minutes prior to any measurements to warm-up and initialise and all measurements are performed in darkness.

2.2 Fluorophore spectroscopy

Fluorophores (NADH, FAD and Protoporphyrin IX (PpIX)) were purchased as powders from Sigma-Aldrich (Gillingham, Dorset, UK) and prepared to 1 M solutions in phosphate buffered saline (PBS). The LAKK-M device was used to measure the fluorescence of the solutions in matte black cuvettes of known optical properties. NADH and FAD were excited at 365 nm and measured across 400–823 nm. PpIX was excited at 635 nm and measured across 650–823 nm.

2.3 Patient recruitment

Ethical approval was obtained from NRES London Central Ethics Committee, UK, for "ABLADE: Diagnosis of bladder cancer using multifunctional laser" (REC reference 14/LO/1076, approved 17.06.14) sponsored by TASC (University of Dundee/NHS Tayside). The ethical approval granted 12 months for the recruitment of 20 patients to the study under informed consent. The inclusion criteria were: patients between the ages of 16–90 with suspected bladder tumour undergoing cystoscopic examination by WLC, with transurethral resection of bladder tumour (TURBT) at Ninewells Hospital, Dundee. Participants were identified and approached solely by the research team. Participants were given a participant information sheet (PIS) and provided informed consent by signing and initialling a consent form.

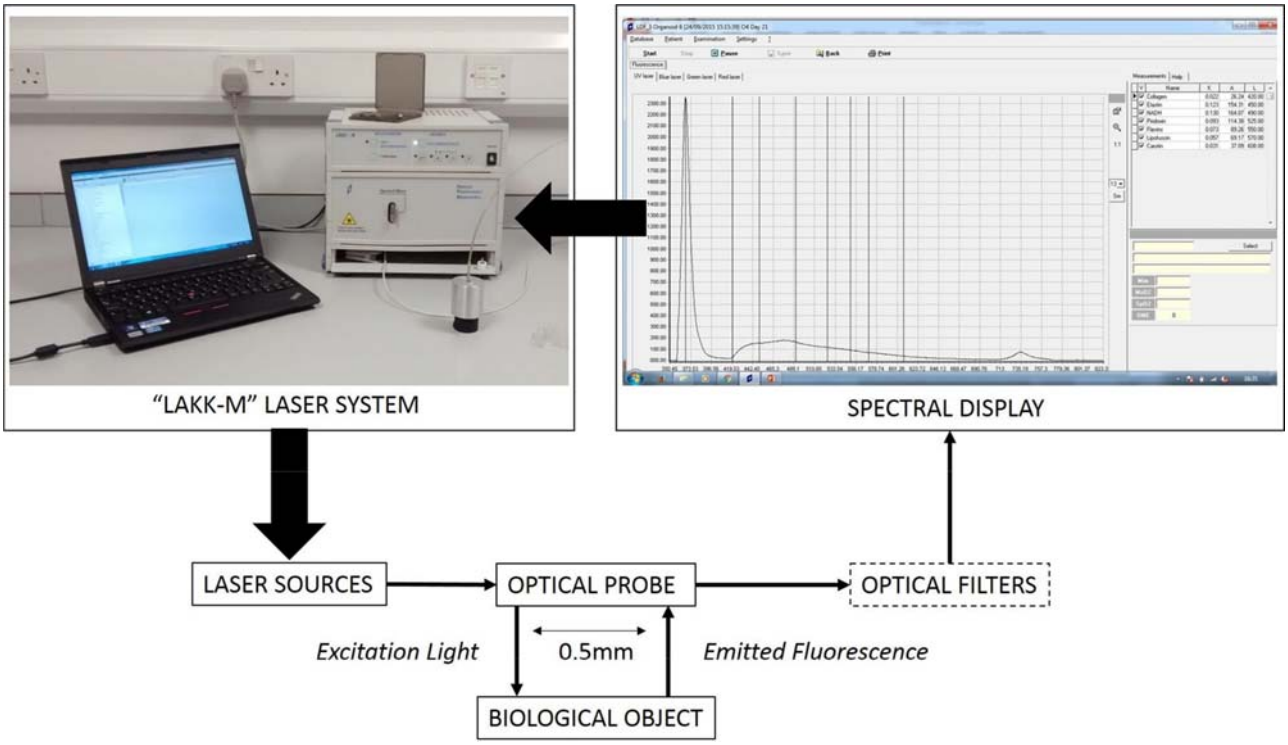

Figure 1 Schematic showing the setup of the LAKK-M laser system and interaction with biological object (biopsy tissue).

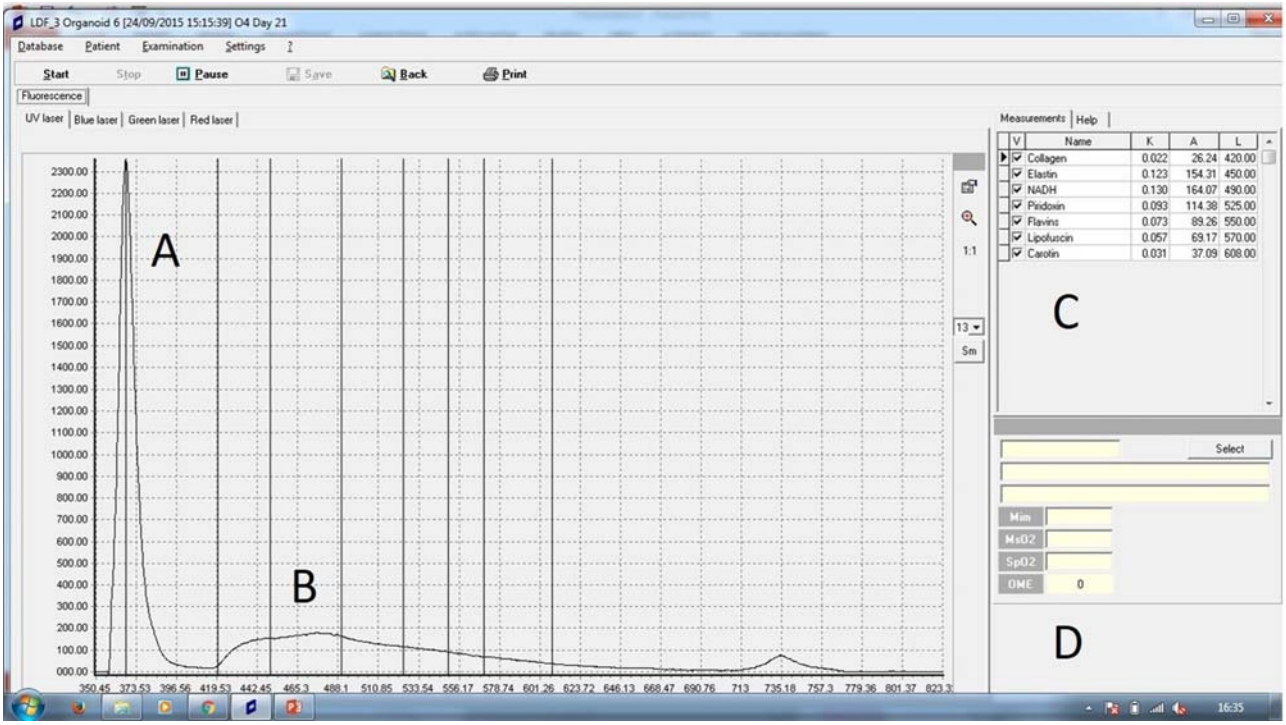

Figure 2 LAKK-M software interface showing the back-scattered laser light (**A**), tissue fluorescence spectrum (**B**), amplitudes of fluorescence for fluorophores of interest (**C**) and calculation of diagnostic ratios (**D**).

2.4 Tissue fluorescence spectroscopy

Tissue was delivered by surgical staff to the research team, either in the workroom adjacent to the urology theatre (in Ninewells Hospital, Dundee), or in the microscopy laboratory (within the Division of Imaging and Technology, University of Dundee, Ninewells Hospital, Dundee). Tissue was placed mucosal side face up where possible (some tissue was obscured by crush and cautery artefacts) in a matte black cuvette of known optical properties. The optical probe of the LAKK-M system was brought into contact with the tissue surface and held for 10 seconds to steady, following which fluorescence spectra were taken from tissue at both 365 nm and 635 nm excitation. One measurement was taken from each sample received, comprising one spectrum excited at 365 nm (UV) and one spectrum excited at 635 nm (red). Often, several samples were received from a similar site on a patient. These were considered as independent samples for the sake of analysis. The 122 (89 cancerous and 33 healthy) entries in the dataset for analysis therefore each represent one measurement of one independent sample. The fluorescence spectra received from tissue were saved in the "LDF 3.1" inbuilt database, denoted by patient ID and by tissue location. The pathology opinion of the tissue was not known to the research team at the time of analysis. Samples were delivered to the lab in closed tissue tubs and measurements were performed in darkness to minimise photo-bleaching. Immediately after analysis, the biopsy samples were delivered to the pathology lab (in Ninewells Hospital, Dundee) by a member of the research team. The process of receiving samples, measuring and returning to the pathology lab took no longer than 2 hours in each instance.

2.5 Histopathology as reference standard

All pathology analyses were independently provided by an experienced, qualified NHS pathologist with no involvement in the research team and no knowledge of the spectroscopy results. From 20 participants, 122 samples were received (therefore 122 independent measurements each of NADH, flavin, ORR and porphyrins). Of the 122 samples, 33 were healthy and 89 were diagnosed as bladder cancer. Of the 33 healthy samples, 10 were normal (non-inflamed) while 23 were inflamed (including cystitis cystica). Within the 89 bladder cancer samples, 6 were CIS, 7 were squamous cell carcinoma (SCC) and 76 were transitional cell carcinoma (TCC). Of the TCC samples: 30 samples were Ta (tumour is contained within the urothelium); 20 were T1 (tumour extends into connective tissue); 26 were T2 (tumour invades into muscle). All 7 of the SCC samples were stage T2.

2.6 Data analysis

Sample spectra were exported as ASCII files and combined, plotted and visualised using Origin Pro 8 analysis software. From the custom-made LDF3.1 software, amplitudes of fluorescence for specific fluorophores of interest were recorded, in keeping with previous work by Dunaev et al. [46], Akbar et al. [47] and Smirnova et al. [48]. The excitation and emission wavelengths for the endogenous fluorophores of interest were as follows (Table 1).

To ensure that porphyrin amplitude of fluorescence was not being affected by measurement angle, tissue turbidity or refractive index, the coefficient of fluorescence contrast (Kf) of porphyrin was also calculated according to previous methods [49] and compared for statistical significance. Fluorescence intensity was also quantified by area under the curve (AUC) calculation to corroborate spectral figures. Sample AUC values were calculated for 365 nm excitation as Σ [I400–823]/5 and for 635 nm excitation as Σ [I650–823]/5. Biomarker amplitude values, porphyrin Kf, ORR (NADH/FAD) and NADH/porphyrin values for each sample, alongside both UV and red AUC values, were collated in a master file using Microsoft Excel, alongside tissue opinion (1 = healthy, 2 = cancer). The study master file was imported to R Studio for statistical analysis. As populations were not normally distributed, populations were compared using the analysis of variance (ANOVA) function in R Studio. Statistical analyses were performed to calculate the p value in every instance, with $p < 0.05$ considered statistically significant. Non-inflamed and inflamed healthy tissue were compared by ANOVA for each parameter. No statistically significant differences were found between populations, therefore they were considered as a single population (healthy) for the purpose of the study. Data were log transformed during analysis to ensure better fit within Q-Q and residuals versus leverage plots. For factors with statistically significant differences between populations, bar charts were generated in Origin Pro 8 depicting the population mean

Table 1 Endogenous fluorophores studied using the LAKK-M system.

Fluorophore	Excitation (nm)	Emission (nm)
NADH	365	490
FAD	365	550
Porphyrin	635	710

± the standard error of the mean (SEM) for opinion (healthy vs cancer). For statistically significant factors, receiver operating characteristic (ROC) curves were generated using Origin Pro 8 analysis software to evaluate the sensitivity/specificity trade-off of a diagnostic parameter at different diagnostic thresholds. For ROC curves, AUC was calculated automatically, with values ranging from 0.5 (worthless) to 1 (excellent).

3. Results and discussion

Average fluorescence spectra from tissue at 365 nm excitation were superimposed over spectra received from 1 M solutions of reduced Nicotinamide Dinucleotide (NADH) and Flavin Adenine Dinucleotide (FAD), excited at 365 nm (Figure 3A). Average fluorescence spectra from tissue at 635 nm were superimposed over spectrum received from 1 M solution of Protoporphyrin 9 (PpIX) excited at 635 nm (Figure 3B). From Figure 3A it can be seen that the spectral shape of tissue under 365 nm excitation suggests a significant contribution from NADH (main tissue peak at 490 nm) and FAD (shoulder peak at 550 nm), while fluorescence spectra of tissue under 635 nm excitation (Figure 3B) suggests a significant contribution from porphyrins (main tissue peak 700–710 nm). Slight differences in full width at half maximum (FWMH) between tissue fluorescence and PpIX may be explained by overlapping fluorescence from the presence of different forms of porphyrin in tissue (coproporphyrin, for example). Differences in line shape of the UV spectra suggested possible differences in ORR values between populations. Furthermore, from the average red fluorescence spectra it can be seen that the intensity of fluorescence from cancer samples is almost double that of healthy tissue. AUC analysis revealed there were no statistically significant differences in total fluorescence intensity (reflected by spectral amplitude) under 365 nm excitation ($p = 0.519$), however there was a statistically significant difference in total fluorescence intensity under 635 nm excitation ($p = 0.00265$). This difference is attributable to the non-normal distribution of tissue fluorescence intensity, which may be more exaggerated at UV wavelengths where blood and other tissue scatterers have a greater effect on measured autofluorescence. Cancer samples were subsequently separated into CIS ($n = 6$), SCC ($n = 7$) and TCC ($n = 76$) cases and plotted alongside healthy and cancer average spectra for both 365 nm excitation (Figure 4A) and 635 nm excitation (Figure 4B). From these figures we can see clearly that the average cancer spectra (red) are largely dictated by contribution from TCC samples (pink) in both cases, as average spectra are almost identical. CIS samples were found to display the lowest average intensity AUC values under 365 nm excitation, while SCC samples displayed the highest. Further observation indicates that the NADH/FAD ratio (ORR) was lowest in CIS and SCC samples. CIS and SCC populations were too small to perform meaningful AUC analysis and therefore would benefit from corroboration in a larger study.

Optical redox ratio (ORR) values for each sample were calculated and compared for statistically significant differences. The mean ± SEM values for healthy and cancerous bladder tissue are depicted below (Figure 5A). A statistically significant decrease in the ORR of cancer tissue compared to healthy can be seen ($p = 0.00891$). This result is in keeping with our previous finding of progressive re-

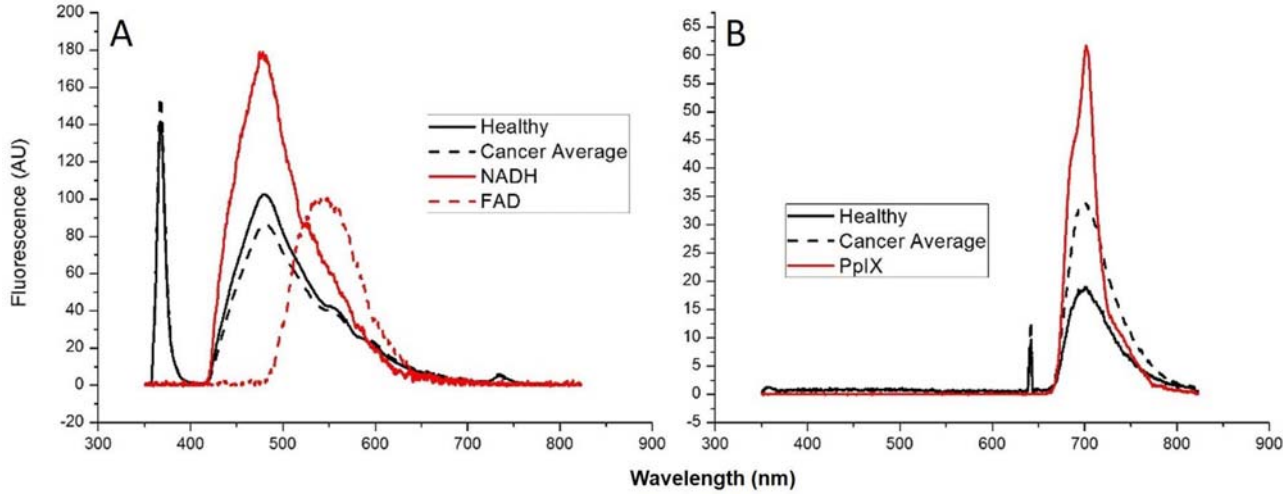

Figure 3 Average fluorescence spectra of healthy (solid black line, $n = 33$) and cancer tissue (dotted black line, $n = 89$) under UV (**A**) and red excitation (**B**): In (**A**), samples are compared with UV fluorescence of NADH (solid red line) and FAD (dotted red line); in (**B**), samples are compared with red fluorescence of Protoporphyrin IX (solid red line).

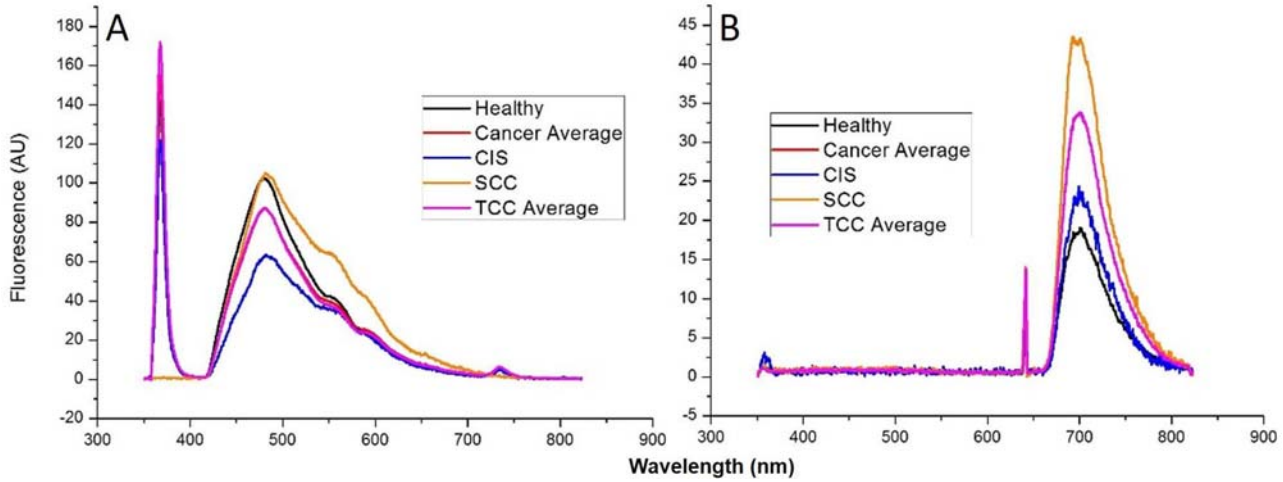

Figure 4 Line graphs charting tissue fluorescence under UV (**A**) and red excitation (**B**) for healthy (black line, n = 33), cancer average (red line, n = 89), CIS (blue line, n = 6), TCC (magenta line, n = 76) and SCC (orange line, n = 7).

ductions in the ORR of bladder cancer organoids. Crucially, this finding reveals that although there were no significant differences in fluorescence intensity, spectral line shape has potential to be employed diagnostically. Small sample number of CIS and SCC tissues prevented meaningful independent analysis, necessitating further study. The amplitude of fluorescence of porphyrins was recorded and analysed for statistically significant differences. The mean ± SEM values for porphyrin fluorescence amplitude in healthy and cancer tissue are depicted below (Figure 5B). From this data it can be seen that porphyrin levels in cancer samples are greatly increased compared to healthy samples. This difference was found to be extremely statistically significant (p = 0.00241). Porphyrin Kf values were also found to be statistically significant (p = 0.0144), indicating tissue optical properties had little effect on porphyrin measurements. From Figure 5C, the average ± SEM values for the NADH/porphyrin ratios for healthy and cancer samples can be seen. The difference between samples was found to be extremely statistically significant (p = 0.00624). ROC curves were generated for all factors to determine their diagnostic worth. Figure 6 below details these ROC curves. From Figure 6A, the UV ORR displays some diagnostic worth for the detection of bladder cancer (AUC value = 0.64), however when comparing healthy samples to CIS samples alone (n = 6) (Figure 6B), the AUC value increases to 0.83, indicating a much more promising diagnostic test. Considering porphyrins (Figure 6C) the AUC value suggests a test with greater diagnostic worth than ORR for all bladder cancers (AUC = 0.71), at the expense of a reduced performance against CIS (AUC = 0.63). Finally, the ROC based on the ratio of NADH to porphyrins (Figure 6D) was found to have an AUC of 0.64. The AUC value for NADH/porphyrin detection of CIS was 0.69.

It was hypothesised that bladder cancer tissue would exhibit a reduced ORR compared to healthy tissue. Furthermore, owing to malfunctions in the heme biosynthetic pathway of cancer cells (the basis of PDD) and previous work by Aboumarzouk et al.

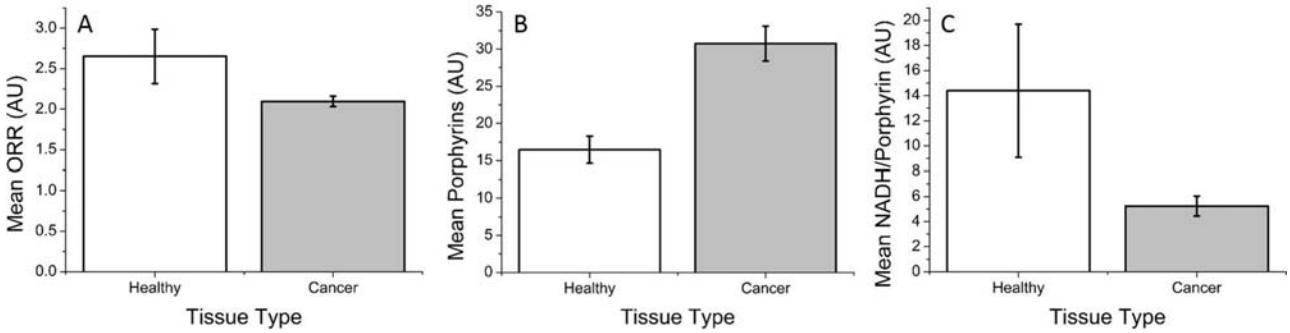

Figure 5 Bar charts showing the average ± SEM values for ORR (**A**), porphyrin amplitude (**B**) and NADH/porphyrin ratio (**C**) values. In each instance, healthy average (n = 33) is depicted in white and cancer average (n = 89) is depicted in grey.

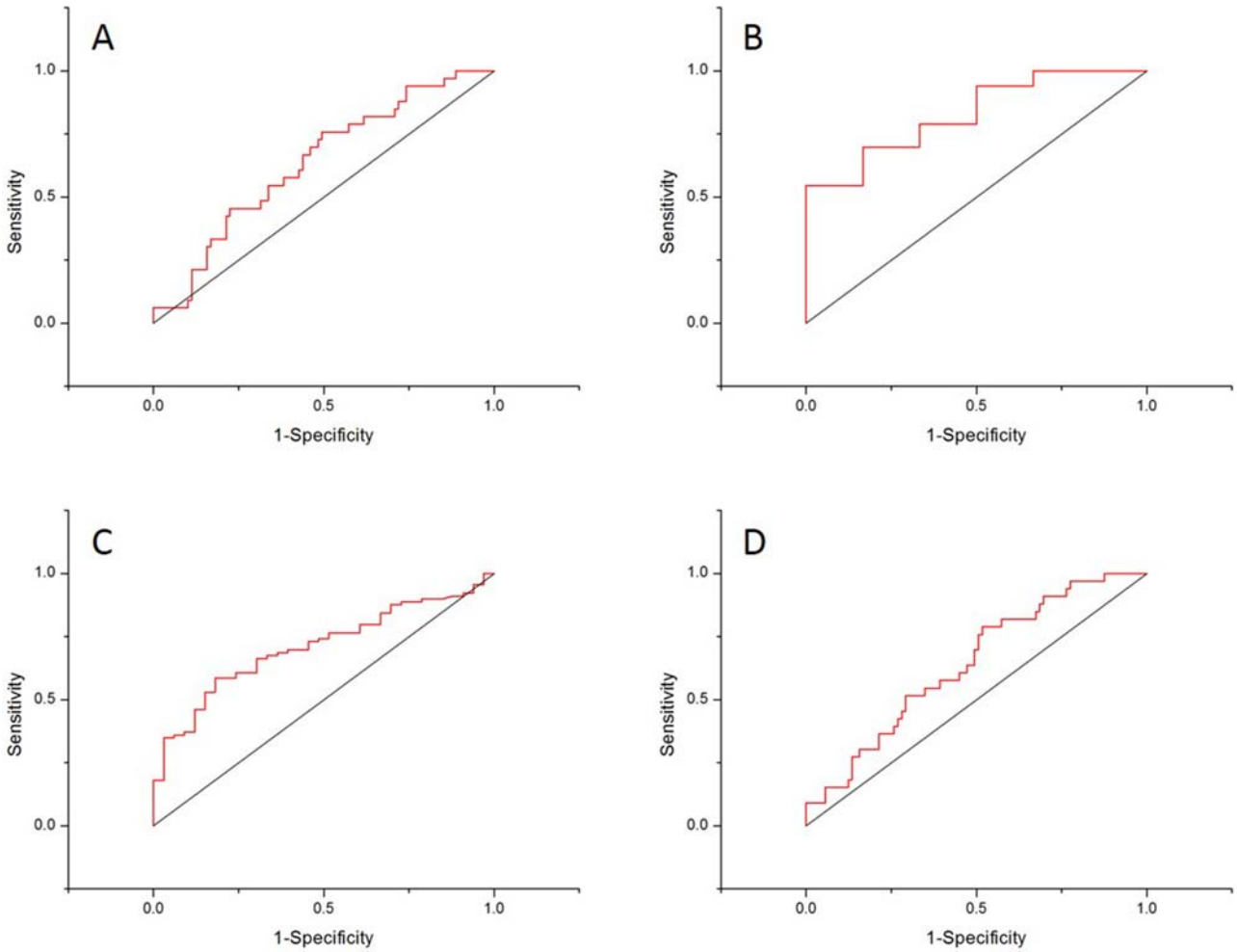

Figure 6 Receiver operating characteristic (ROC) curves depicting the diagnostic accuracy (1-specificity vs. sensitivity) of UV ORR (**A**), UV ORR for just CIS samples (**B**), porphyrin amplitude (**C**) and NADH/porphyrin ratio (**D**).

[35], it was hypothesised it would be possible to detect an elevated level of endogenous porphyrins and a reduced NADH/porphyrin ratio in cancer tissue compared to healthy control. Results confirm these hypotheses. Firstly, it was demonstrated that tumours exhibit a reduced ORR compared to healthy tissue. This is in keeping with our own previous findings in an organoid model of bladder cancer [42]. Most contemporary focus on the ORR suggests that the metabolic alterations which occur during cancer development skew the degree to which cancer cells use their electron transport chain, thus causing accumulation of NADH in cancer cells. We ourselves have previously confirmed this finding in bladder cancer cell lines [28], however the ORR has not been extensively covered regarding human bladder tissue. At the tissue level other fluorophores may contribute to the complex fluorescence spectrum obtained under UV (365 nm) illumination, such as the structural proteins collagen and elastin, although the spectral overlap from these proteins past 450 nm was shown to be minimal [50]. Previously, Mayevsky et al. described a multi-parametric sensing system similar to the LAKK-M, using it to study NADH fluorescence up to 480 nm [51] so we consider that this is the major contributing fluorophore up to 500 nm. Comparisons between average tissue fluorescence under UV illumination and the endogenous fluorophores NADH and FAD confirm that these are the major contributing fluorophores to tissue fluorescence at this wavelength, indicated by the lack of definitive tissue fluorescence peaks <490 nm. ROC curve analysis of the ORR suggests it displays some potential as a diagnostic tool, but is particularly effective at detecting CIS (based on a small sample number). CIS is commonly missed during WLC and displays potential to progress into MIBC, therefore new techniques for its detection are crucial. Particular effectiveness for the ORR in detecting CIS also suggests this phenomenon is independent of tissue thickening. Future studies should therefore seek to corroborate these findings regarding the ORR, with

a particular focus on an increased population of CIS samples.

Tissue photo-bleaching and fading is a common concern in tissue spectroscopy, caused by the exhaustion of tissue fluorophores by irradiating light (specific and non-specific) [52]. NADH is a particular subject of photo-bleaching in tissue [53]. To overcome the non-specific photo-bleaching of tissue autofluorescence in our study, samples were transported to the analysis lab and measured in complete darkness. Each sample was irradiated by low power lasers (<6 mW) for at most 10 seconds, thereby minimising photo-bleaching. As all samples were measured identically, the effects of photo-bleaching will have a minimal effect on our results. Furthermore, tissue NADH autofluorescence is known to alter after tissue has been removed from the body. This is due to the removal of blood supply and oxygenation from excised tissue, altering its metabolic profile. Anoxic and hypoxic conditions have been shown to cause increases in relative NADH fluorescence (reviewed by Mayevsky et al. [54]). NADH and ORR values are therefore likely altered *ex vivo* compared to *in vivo* analyses, however this is not a methodological concern for our study. As all samples analysed in this study (both healthy and cancer) were processed and measured identically, and all analyses were carried out <2 hours post resection, we consider that the phenomenon of NADH fluorescence alteration should have minimal impact on our findings *ex vivo* as we directly compared the two populations. We assume that NADH perturbation occurs at similar rates in healthy and cancerous tissue, although future studies should seek to corroborate this. Future *ex vivo* analysis using the same technique may benefit from storing excised tissue in culture media, as this has been shown to maintain tissue autofluorescence profiles up to 4 hours post-excision [55]. The application of this technique *in vivo* should take into account the changes to NADH autofluorescence in excised tissue. *In vivo,* tissue may be expected to display significantly different fluorescence intensities alongside altered ORR values. Future studies may benefit from directly comparing the same bladder samples measured *in vivo* and *ex vivo* at various time points to improve understanding of NADH dynamics.

Our findings in this paper contrast our previous findings of elevated ORR at the cellular level [28], however they may be a result of metabolic abnormalities across a range of different cell types, including cancer cells themselves and surrounding healthy urothelium and fibroblasts. Regarding porphyrin levels, the statistically significant increase in porphyrin levels in cancer tissue suggests a selective accumulation similar to that which is witnessed in PDD but without the need for PS administration. Furthermore, ROC calculations suggest that this biomarker possesses potential for diagnosis. One of the largest limitations to PDD is its reduced specificity. In particular, inflamed benign tissue is often recorded as cancer under PDD, owing to the leaky vasculature of tissue previously treated by chemotherapy or surgery. This results in increased false positive rates and a number of unnecessary invasive biopsies. That a statistically significant difference in endogenous porphyrin levels between healthy (including inflamed tissue) and cancer was observed suggests in future it may be possible to quantify porphyrin levels in non-sensitised tissue with the ability to discern between inflamed and cancer tissue. Endogenous porphyrins have previously been shown to be measurable at low levels across most aerobic human tissue [56], being excreted in the urine. Increased endogenous porphyrin levels have previously been observed in renal cell carcinoma [45]. Similarly, iron levels (the ultimate product of the porphyrin biosynthetic pathway) have been shown to preferentially accumulate in mouse mammary tumours [57] where they have been suggested to play a role in tumour cell survival and progression. Endogenous porphyrin fluorescence has previously been described in non-sensitised oral mucosa, even in healthy tissue [58]. Oral mucosa possesses similar structure to that of the bladder, therefore we consider that non-sensitised healthy bladder would likewise present some endogenous porphyrin fluorescence. In order to better exploit the tissue optical window and avoid fluorescence contributions from other fluorophores at lower wavelength (for instance, FAD and lipofuscin at 405 nm), we studied the secondary porphyrin peak at 635 nm excitation/710 nm emission. This is in keeping with previous work in oral mucosa – in which identical measurement parameters observed increased endogenous porphyrin fluorescence in tumour tissue with small fluorescence signal from healthy tissue [49] – and in PDD of bladder TCC [59]. Average fluorescence from both tumour and healthy tissue was low under red excitation, compared with tissue fluorescence under UV excitation, reflecting small but detectable concentration of porphyrin in non-sensitised bladder tissue. In addition to intensity of porphyrin fluorescence, we also observed statistically significant differences in coefficient of fluorescent contrast (Kf) for porphyrin values between healthy and cancer, indicating that differences are due to fluorescence as opposed to other factors such as tissue refractive index, turbidity, etc. Previously, it has been suggested that chronic hypoxia is un underlying factor of increased porphyrin levels in oral mucosa [49], therefore the elevated porphyrin level and, more importantly, the reduced NADH/porphyrin values observed in bladder cancer may reflect an effect of tissue hypoxia on the reduction of cell metabolic activity. One concern for the application of our technique is its low applicability

to CIS detection in a small sample size. Theoretically, the use of longer wavelengths of light to investigate tissue should allow deeper penetration into tissue and the detection of a greater number of flat lesions (for instance, CIS), therefore it may be that the metabolic perturbations resulting in increased porphyrin levels in obvious bladder cancer are not at play in pre-cancerous lesions. Finally, NADH/porphyrin levels were observed to be decreased in cancer samples, in keeping with previous research findings [35].

Uncertainty of presented average spectra is another common concern when disseminating spectrometric findings. To address this we performed AUC analysis on spectra excited from tissue excited at 365 nm and 635 nm. In keeping with previous research in the field, average UV (365 nm) induced fluorescence AUC value was greater in healthy tissue than in cancer, however this was not statistically significant. This could be due to the effects of tissue thickness on amplitude of fluorescence (which ranged from 2–15 mm) and also angle and firmness of application of the diagnostic probe to tissue. AUC analysis of 635 nm excited tissue spectra revealed a statistically significant difference, reflecting the robustness of the presented spectra. Diagnostic ratios such as the ORR and NADH/Porphyrin ratio are less affected by these factors and are therefore more robust measurements for diagnosis. This study has not only corroborated previous findings by ourselves [42] and others [35] but also applied findings from other forms of cancer [45] to the identification of a novel biomarker for bladder cancer (endogenous porphyrins). As this was a pilot study of 20 participants, it would be of worth to expand this study with particular focus on diagnostic ratios such as ORR and NADH/porphyrins with particular focus on their applicability to CIS and early stage tumours. The LAKK-M system has not previously been used for the study of bladder cancer tissue, however understanding of the autofluorescence of bladder cancer [33, 60] and development of the LAKK-M for the study of fluorophore variability in healthy volunteers [46] and the diagnosis of cardiovascular disease [47] suggests its worth as a diagnostic tool. Furthermore, efforts are ongoing to better understand the bladder tissue fluorescence spectra in health and disease by using tissue fluorescence simulation models [61, 62]. Combination of fluorescence data with tissue simulations will allow delineation of the contribution of fluorophores such a NADH, FAD and collagen to recorded fluorescence. The LAKK-M system also contains sources for laser Doppler flowmetry (LDF) and tissue reflectance oximetry (TRO) which have previously been assessed from a diagnostic perspective [63]. LDF has been used to identify and characterise interstitial cystitis [64] while tumour hypoxia is a much-studied subject [65]. Identification and substantiation of suitable biomarkers of bladder cancer using the autofluorescence spectroscopy channel may allow the LAKK-M system to be developed into an effective multi-functional diagnostic tool for bladder cancer.

Application of the LAKK-M system for *in vivo* study and clinically will rely on a number of modifications to the system. The design of the LAKK-M system – with a central functional unit and external optical probe – is well suited to clinical application. The optical probe containing the excitation and detection fibres is roughly 1 M in length, therefore it should theoretically be suitable for trans-urethral application. A limitation to the system is its lack of imaging capability, relying instead on spectral readouts. For this reason, clinical application of the system should be done so alongside white light cystoscopy to give the research team a better visualisation of tissue. One further limitation to the LAKK-M system is the measurement geometry. In order to receive useful diagnostic information, the optical probe must be brought gently into contact with the tissue of interest. This may be afforded by conjunction with a rigid or flexible cystoscope. Previously, Aboumarzouk et al. described a setup using the WavSTAT system, whereby a clamping device holds the probe in place during spectral analysis [35]. A similar setup may be employed with the LAKK-M optical probe to ensure sufficient contact between probe and tissue. The diameter of the outer assembly of the optical probe (2 mm) should fit within the narrow confines of the urethra, even alongside a cystoscope, although the optical probe is modifiable to the addition or removal of unnecessary fibres (for instance, the probe diameter could be minimised by removing all but the 365 nm and 635 nm sources and detector). Finally, cystoscopic application necessitates sterilisation to avoid infection, which may be afforded by disposable sheaths to cover the optical probe. These modifications would allow the LAKK-M system to be applied in a clinical setting.

4. Conclusion

In conclusion, this pilot study into the autofluorescence profiles of healthy and cancerous human bladder tissue using the MLNDS "LAKK-M" has identified three main parameters with which to detect bladder cancer. These findings improve understanding of the contribution and dynamics of several endogenous fluorophores to bladder cancer fluorescence spectra, identifying potential novel biomarkers with which to detect the disease. The LAKK-M system had not previously been used to study bladder cancer, however these findings present immense promise for the system to be developed into a multi-

functional minimally invasive system for the diagnosis of the disease. The findings presented in this pilot study would benefit from corroboration in a large scale study, with particular focus on the discrimination of CIS.

Acknowledgements This work was funded through the European Union 7th Framework Programme (EU FP7) project "ABLADE: Advanced bladder cancer diagnosis and therapy" (grant agreement number 324370), with studentship stipend contributions from the NHS and EPSRC (grant number EP/K503010/1). There was further financial contribution from the state task of the Ministry of Education and Science, Russian Federation, for the State University – Education-Science-Production complex (basic part, No 310). We acknowledge the contribution of the NHS urology theatre and surgical staff for their assistance with this study and the urology secretaries for assistance in identifying participants, and would also like to thank Professor Steve Hubbard, School of the environment, University of Dundee, for statistical analysis advice. Full datasets supporting this publication can be found at the following DOI: 10.15132/10000115.

Author biographies Please see Supporting Information online.

References

[1] CRUK, Bladder cancer statistics. 2016; http://www.cancerresearchuk.org/health-professional/cancer-statistics/statistics-by-cancer-type/bladder-cancer. Accessed 21.04.16, 2016.
[2] P. A. Humphrey, J. Urol. **187**(3), 1057–1058 (2012).
[3] P. S. Sullivan, J. B. Chan, M. R. Levin, and J. Rao, Am. J. Transl. Res. **2**(4), 412–440 (2010).
[4] R. Talwar, T. Sinha, S. C. Karan, D. Doddamani, A. Sandhu, G. S. Sethi, A. Srivastava, V. Narang, A. Agarwal, and N. Adhlakha, Urology **70**(2), 267–271 (2007).
[5] F. A. Yafi, F. Brimo, J. Steinberg, A. G. Aprikian, S. Tanquay, and W. Kassouf, Urol. Uncol. **33**(2), 25–31 (2015).
[6] B. L. Isfoss, BJU Int. **108**(11), 1703–1707 (2011).
[7] G. Mowatt, J. N'Dow, L. Vale, G. Nabi, C. Boachie, J. A. Cook, C. Fraser, and T. R. Griffiths, Aberdeen Technology Assessment Review (TAR) Group, Int. J. Technol. Assess. Health Care **27**(1), 3–10 (2011).
[8] H. Ren, K. C. Park, R. Pan, W. C. Waltzer, K. R. Shroyer, and Y. Pan, J. Urol. **187**(3), 1063–1070 (2012).
[9] D. J. Parekh, B. H. Bochner, and G. Dalbagni, J. Clin. Oncol. **24**(35), 5519–5527 (2006).
[10] H. Maeda, Adv. Enzyme Regul. **41**, 189–207 (2001).
[11] J. E. Frampton and G. L. Plosker, Drugs **66**(4), 571–578 (2006).
[12] K. Inoue, U. Ota, M. Ishizuka, C. Kawada, H. Fukuhara, T. Shuin, I. Okura, T. Tanaka, and S. Ogura, Photodiagnosis Photodyn. Ther. **10**(4), 484–489 (2013).
[13] M. Burger, H. B. Grossman, M. Droller, J. Schmidbauer, G. Hermann, O. Dragoescu, E. Ray, Y. Fradet, A. Karl, J. P. Burgues, J. A. Witjes, A. Stenzl, P. Jichlinski, and D. Jocham, Eur. Urol. **64**(5), 846–854 (2013).
[14] A. Stenzl, M. Burger, Y. Fradet, L. A. Mynderse, M. S. Soloway, J. A. Witjes, M. Kriegmair, A. Karl, Y. Shen, and H. B. Grossman, J. Urol. **184**(5), 1907–1913 (2010).
[15] M. C. Grimbergen, C. F. van Swol, T. G. Jonges, T. A. Boon, and R. J. van Moorselaar, Eur. Urol. **44**(1), 51–56 (2003).
[16] A. B. Ghisaidoobe and S. J. Chung, Int. J. Mol. Sci. **15**(12), 22518–22538 (2014).
[17] L. Zhang, Y. Pu, J. Xue, S. Pratavieira, B. Xu, S. Achilefu, and R. R. Alfano, J. Biomed. Opt. **19**(3), 37005 (2014).
[18] V. Prabhu, S. B. Rao, E. M. Fernandes, A. C. Rao, K. Prasad, and K. K. Mahato, PLoS One **9**(5), e98609 (2014).
[19] P. L. Tong, J. Qin, C. L. Cooper, P. M. Lowe, D. F. Murrell, S. Kossard, L. G. Ng, B. Roediger, W. Weninger, and N. K. Haass, Br. J. Dermatol. **169**(4), 869–879 (2013).
[20] K. Drozdowicz-Tomsia, A. G. Anwer, M. A. Cahill, K. N. Madlum, A. M. Maki, M. S. Baker, and E. M. Goldys, J. Biomed. Opt. **19**(8), 086019 (2014).
[21] J. Horilova, B. Cunderlikova, and A. Marcek Chorvatova, J. Biomed. Opt. **20**(5), 51017 (2015).
[22] L. C. Courrol, F. R. de Oliveira Silva, E. L. Coutinho, M. F. Piccoli, R. D. Mansano, N. D. Vieira Jr., N. Schor, and M. H. Bellini, J. Fluoresc. **17**(3), 289–292 (2007).
[23] H. Sato and T. Takino, Cancer Sci. **101**(4), 843–847 (2010).
[24] M. G. Vander Heiden, L. C. Cantley, and C. B. Thompson, Science **324**(5930), 1029–1033 (2009).
[25] A. Varone, J. Xylas, K. P. Quinn, D. Pouli, G. Sridharan, M. E. McLaughlin-Drubin, C. Alonzo, K. Lee, K. Munger, and I. Georgakoudi, Cancer Res. **74**(11), 3067–3075 (2014).
[26] Q. Liu, G. Grant, J. Li, Y. Zhang, F. Hu, S. Li, C. Wilson, K. Chen, D. Bigner, and T. Vo-Dinh, J. Biomed. Opt. **16**(3), 037004 (2011).
[27] J. H. Ostrander, C. M. McMahon, S. Lem, S. R. Millon, J. Q. Brown, V. L. Seewaldt, and N. Ramanujam, Cancer Res. **70**(11), 4759–4766 (2010).
[28] S. Palmer, K. Litvinova, E. U. Rafailov, and G. Nabi, Biomed. Opt. Express **6**(3), 977–986 (2015).
[29] R. R. Alfano, B. B. Das, J. Cleary, R. Prudente, and E. J. Celmer, Bull N Y Acad. Med. **67**(2), 143–150 (1991).
[30] R. R. Alfano, D. Tata, J. Cordero, P. Tomashefsky, F. Londo, and M. Alfano, IEEE J. Quant. Electr. **20**, 1507–1511 (1984).
[31] N. Ramanujam, Neoplasia **2**(1–2), 89–117 (2000).
[32] M. A. D'Hallewin, L. Baert, and H. Vanherzeele, J. Am. Paraplegia Soc. **17**(4), 161–164 (1994).

[33] W. Zheng, W. Lau, C. Cheng, K. C. Soo, and M. Olivo, Int. J. Cancer **104**(4), 477–481 (2003).
[34] C. Schafauer, D. Ettori, M. Roupret, V. Phe, J. M. Tualle, E. Tinet, S. Avrillier, C. Egrot, O. Traxer, and O. Cussenot, J. Urol. **190**(1), 271–277 (2013).
[35] O. Aboumarzouk, R. Valentine, R. Buist, S. Ahmad, G. Nabi, S. Eljamel, H. Moseley, and S. G. Kata, Photodiagnosis Photodyn. Ther. **12**(1), 76–83 (2015).
[36] I. Rokahr, S. Andersson-Engels, S. Svanberg, M. D'Hallewin, L. Baert, I. Wang-Nordman, and K. Svanberg, Proc. SPIE **2627**, 2 (1995).
[37] M. A. D'Hallewin, L. Bezdetnaya, and F. Guillemin, Eur. Urol. **42**, 417–425 (2002).
[38] Y. Pu, W. Wang, G. Tang, and R. R. Alfano, J. Biomed. Opt. **15**(4), 047008 (2010).
[39] I. Georgakoudi, B. C. Jacobson, M. G. Muller, E. E. Sheets, K. Badizadegan, D. L. Carr-Locke, C. P. Crum, C. W. Boone, R. R. Dasari, J. Van Dam, and M. S. Feld, Cancer Res. **62**(3), 682–687 (2002).
[40] R. Drezek, K. Sokolov, U. Utzinger, I. Boiko, A. Malpica, M. Follen, and R. Richards-Kortum, J. Biomed. Opt. **6**(4), 385–396 (2001).
[41] M. Anidjar, O. Cussenot, S. Avrillier, D. Ettori, J. M. Villette, J. Fiet, P. Teillac, and A. Le Duc, J. Biomed. Opt. **1**(3), 335–341 (1996).
[42] S. Palmer, K. Litvinova, A. Dunaev, S. Fleming, D. McGloin, and G. Nabi, Biomed. Opt. Express **7**(4), 1193–1200 (2016).
[43] L. Shi, A. Rodriguez-Contreras, Y. Budansky, Y. Pu, T. A. Nguyen, and R. R. Alfano, J. Biomed. Opt. **19**(6), 066009 (2014).
[44] M. Inaguma and K. Hashimoto, Cancer **86**(11), 2201–2211 (1999).
[45] M. H. Bellini, E. L. Coutinho, L. C. Courrol, F. Rodrigues de Oliveira Silva, N. D. Vieira Jr., and N. Schor, J. Fluoresc. **18**(6), 1163–1168 (2008).
[46] A. V. Dunaev, V. V. Dremin, E. A. Zherebtsov, I. E. Rafailov, K. S. Litvinova, S. G. Palmer, N. A. Stewart, S. G. Sokolovski, and E. U. Rafailov, Med. Eng. Phys. **37**(6), 574–583 (2015).
[47] N. Akbar, S. Sokolovski, A. Dunaev, J. J. Belch, E. Rafailov, and F. Khan, J. Microsc. **255**(1), 42–48 (2014).
[48] O. D. Smirnova, D. A. Rogatkin, and K. S. Litvinova, J. Innov. Opt. Health Sci. **5**(2), 1–9 (2012).
[49] K. S. Litvinova, D. A. Rogatkin, O. A. Bychenkov, and V. I. Shumskiy, Proc. SPIE **7547**, Saratov fall meeting (2009).
[50] A. C. Croce and G. Bottiroli, Eur. J. Histochem. **58**(4), 2461 (2014).
[51] A. Mayevsky and B. Chance, Mitochondrion **7**(5), 330–339 (2007).
[52] H. Zeng, C. MacAulay, D. I. McLean, B. Palcic, and H. Lui, Photochem. Photobiol. **68**(2), 227–236 (1998).
[53] L. M. Tiede and M. G. Nichols, Photochem. Photobiol. **82**(3), 656–664 (2006).
[54] A. Mayevsky and G. G. Rogatsky, Am. J. Physiol. Cell Physiol. **292**(2), 615–640 (2007).
[55] A. J. Walsh, K. M. Poole, C. L. Duvall, and M. C. Skala, J. Biomed. Opt. **17**(11), 116015 (2012).
[56] K. Koenig and H. Schneckenburger, J. Fluoresc. **4**(1), 17–40 (1994).
[57] I. Freitas, E. Boncompagni, R. Vaccarone, C. Fenoglio, S. Barni, and G. F. Baronzio, Anticancer Res. **27**(5A), 3059–3065 (2007).
[58] D. M. Harris and J. Werkhaven, Lasers Surg. Med. **7**(6), 467–472 (1987).
[59] S. N. Datta, C. S. Loh, A. J. MacRobert, S. D. Whatley, and P. N. Matthews, Br. J. Cancer **78**(8), 1113–1118 (1998).
[60] F. Koenig, F. J. McGovern, A. F. Althausen, T. F. Deutsch, and K. T. Schomacker, J. Urol. **156**(5), 1597–1601 (1996).
[61] I. Rafailov, S. Palmer, K. Litvinova, V. Dremin, A. Dunaev, and G. Nabi, Proceedings SPIE, San Francisco, USA, 2015, Photonic Therapeutics and Diagnostics XI, 93030W (2015).
[62] I. E. Rafailov, V. V. Dremin, K. S. Litvinova, A. V. Dunaev, S. G. Sokolovski, and E. U. Rafailov, J. Biomed. Opt. **21**(2), 25006 (2016).
[63] A. V. Dunaev, V. V. Sidorov, A. I. Krupatkin, I. E. Rafailov, S. G. Palmer, N. A. Stewart, S. G. Sokolovski, and E. U. Rafailov, Physiol. Meas. **35**(4), 607–621 (2014).
[64] P. Irwin and N. T. Galloway, J. Urol. **149**(4), 890–892 (1993).
[65] W. R. Wilson and M. P. Hay, Nat. Rev. Cancer **11**(6), 393–410 (2011).